Bull. Mater. Sci., Vol. 39, No. 1, February 2016, pp. 79–84. © Indian Academy of Sciences.

Investigation of TaC–TaB_2 ceramic composites

BEHZAD MEHDIKHANI[1,*], GHOLAM HOSSEIN BORHANI[1], SAEED REZA BAKHSHI[1] and HAMID REZA BAHARVANDI[2]

[1]Department of Materials Engineering, Malek-e-Ashtar University of Technology, Isfahan, Iran
[2]Department of Materials Engineering, Malek-e-Ashtar University of Technology, Tehran, Iran

MS received 28 July 2015; accepted 19 October 2015

Abstract. **The TaC–TaB_2 composition was sintered by spark plasma (SPS) at 1900–2100°C and applied pressure of 30 MPa. TaC and 2–3 wt% B_4C were used as starting powders. Densification process, phase evolution, microstructure and the mechanical properties of the composites were investigated. The results indicated that the TaC–TaB_2 composition could be SPS to 97% of theoretical density in 10 min at 2100°C. Addition of B_4C leads to an increase in the density sample from 76 to 97%. B_4C nano-powder resists grain growth even at high temperature 2100°C. The formation of TaB_2/carbon at TaC grain boundaries helps in pinning the grain boundary and inhibiting grain growth. The phase formation was associated with carbon and boron diffusion from the starting particles B_4C to form TaB_2 phases. TaC grain sizes decreased with increase in B_4C concentration. Samples with 2.0 wt% B_4C composition had highest flexure strength up to 520 MPa. The effect of B_4C addition on hardness measured by microhardness has been studied. Hardness of samples containing 3.0 wt% B_4C was 16.99 GPa.**

Keywords. **TaC–TaB_2; spark plasma sintering; hardness; flexure strength; microstructure.**

1. Introduction

Tantalum carbide and boride are an important ultra-high temperature ceramic (UHTC) for potential applications at >2000°C [1]. These materials have attracted interest in recent years due to the increased demand for higher performance materials for applications in extremely harsh environments, such as propulsion systems for future hypersonic vehicles [2–5]. Tantalum carbide ceramics are difficult to densify because of the rapid grain growth of TaC_y [6–8], which leads to entrapped porosity. One of the methods to inhibit grain growth is by reductive agents such as C and B_4C to eliminate the oxides impurities [8]. These impurities [7,8] resulted in enhanced TaC grain growth during densification, which could be due to liquid phase formation, evaporation condensation or other mechanisms. Other beneficial approaches included using extremely fine starting powders [9,10] or adding a UHTC diboride to physically pin grain growth [7]. Another method for increasing the final density is reducing the particle size of the powders. Research shows that finer powder produces a higher final density than coarser powder, particularly when decreasing from the micrometre to the nanometre scale [11]. This indicates that starting with nanoscale powders would be beneficial in sintering TaC, which is normally difficult to densify. However, research by Sommer *et al* [12] shows that rapid grain growth can occur (from 100 to 500 nm) during conventional sintering, particularly in carbide ceramics. Kim *et al* [13] have shown that initial particle size is essential to the final density of TaC during high heating rate experiments, with larger particle size indicating a lower final density. Another method for increasing the final density is by spark plasma sintering (SPS). Spark plasma sintering is a relatively novel consolidation method that has the advantage of short sintering duration and has shown better densification and properties than hot pressing. SPS has been extensively used for synthesis of UHTCs and their composites [2]. Optimization of sintering conditions and microstructural parameters led to the following mechanical property: flexural strength ranging from 670 to 900 MPa for TaC-based ceramics [14]. In this work, the densification, microstructure, mechanical properties of TaC–TaB_2 composites were investigated. In this study, 2–3 wt% B_4C was added to reaction (1) and modified it by:

$$2TaC + B_4C \rightarrow 2TaB_2 + 3C. \quad (1)$$

The main novelty of this work is the use of synthesized nanometric powders and discussion about TaC–TaB_2 composites.

2. Experimental

2.1 *Raw material*

The raw material characteristics are listed in table 1. Purity of TaC powder was higher than 99%. The main impurities were 0.3 wt% Nb, 0.1 wt% Fe, 0.20 wt% O, 0.15 wt% free carbon, 0.05 wt% N, and Al, Ca, K, Na, Ti with a total amount <0.05 wt%. B_4C was >95 wt% pure with major impurities of

*Author for correspondence (Beh_mehdikhani@yahoo.com)

free carbon. Preparation and properties of the powders were the same as detailed in previous paper [15].

2.2 *Spark plasma sintering*

Spark plasma sintering (SPS) was utilized to consolidate TaC–B_4C and TaC–TaB_2 powders. SPS was carried out in Argon atmosphere at 1900 to 2100°C. The heating rate of 100°C min^{-1} was adopted to reach the maximum temperature with a hold time of 10 min. SPS was carried out at 30 MPa pressure. The powders were pressed in graphite dies and punches with approximately 4–5 mm thick and 15 mm in diameter. In this work, to prevent the sticking of powder to dies, graphite foil was used around the powders. Theoretical density for the sintered composites was determined by the law of mixtures. Bulk densities were measured by the Archimedes method. Relative density and open porosity were calculated. Phase compositions were analysed by X-ray diffraction (XRD). The lattice parameter (a) for the cubic TaC_y was calculated by refining the XRD. The C/Ta ratio in the TaC_y was determined according to equation (2) given by Storms [8].

$$C/Ta = -25.641 + 5.9757a_0 \quad (2)$$

Microhardness was measured using Vickers' indentation (Model 3202, zwick) by applying a load of 2.0 kg (19.6 N). To measure three-point flexural strength, the specimens were cut in dimensions 1 × 0.5 cm and their edges were polish for elimination of micro-cracks. Three-point bending strength was measured in a mechanical load frame (SANAF-1 TON). This machine has delicate jaw for small samples. Microstructure was observed by field-emission scanning electron microscopy (FE-SEM). The samples were sectioned, ground and were polished to 1 μm diamond finish.

3. Result and discussion

XRD spectra, phase assembles, relative density (%), lattice parameter (Å) and the calculated C/Ta ratios for cubic TaC_y in the TaC/TaB_2 composites SPS for 10 min at different temperatures are shown in table 2.

Table 1. Raw material characteristics.

Material	Purity	Particle size	Supplier
TaC	99%	1.25 μm	Ningxia Orient
B_4C	>95 wt%	300 nm	Jingangzuan

3.1 *XRD and thermodynamic calculation*

Figure 1 exhibits predominant cubic TaC_y, hexagonal TaB_2 and carbon. No other crystalline phases (if present) were revealed in the XRD spectra to the detecting limit of XRD. This meant the B_4C particle had completely decomposed, and B and C were incorporated into the TaC lattice to form TaC_y and TaB_2, despite of some B and C loss by reducing oxide impurities [8,16]. TaC in the starting powder had regulated its stoichiometry and contributed part of the TaC_y contents. A commercial software program (HSC Chemistry, Fairfield, CA, USA) was used to identify the probable reaction using thermodynamic data. The change in standard Gibbs free energy (ΔG°) indicated that reaction (1) was favourable across the range of processing temperatures, which suggested that B_4C reacted with TaC to form TaB_2 and C:

$\Delta G^\circ = -66.4 + 0.0103T$ (kJ) favourable across the processing temperature range. TaC is not chemically compatible with B_4C. For the overall composition produced by adding relatively small amounts of B_4C to TaC, the phase diagram indicated that TaB_2 and C were stable with TaC [15]. Analysis of the XRD patterns (figure 1) showed a progressive increase in the amount of the TaB_2 phase formed during SPS when the B_4C addition was increased from 2.0 to 3.0 wt%. The amounts of TaB_2 formed could be as high as 14.0 wt% for a B_4C addition of 2.0 and 22.0 wt% for a B_4C addition of 3.0 wt%, if all of the B_4C were consumed by reaction (1). Rietveld refinement of XRD patterns shows that when 2.0 wt% B_4C was added, spark plasma sintered ceramic contained 89 wt% TaC and 11 wt% TaB_2. When 3.0 wt% B_4C was added, the spark plasma sintered ceramic contained 82.0 wt% TaC and 18.0 wt% TaB_2. The amounts of TaB_2 detected by XRD were less than the stoichiometric amounts predicted using reaction (1), indicating that some of the B_4C had reacted with surface oxides (e.g., Ta_2O_5) instead of TaC. The relative densities of the materials were significantly improved by increasing the SPS temperature from 1900 to 2100°C (table 2).

TaC without additive and TaC–2.0 wt% B_4C after sintering at 1900°C had relative density of 66 and ∼76%. B_4C in these samples cause density increase at same temperature. When the SPS was increased to 1900°C or above, the open

Table 2. Relative density, phase assemble and lattice parameter of the TaC–B_4C composites.

Samples	Sintering temperature (°C)	Theoretical density (g cm^{-3})	Relative density (%)	Lattice parameter (Å)	TaC_y C/Ta
TaC	1900	14.3	66	4.448	0.9389
TaC–2 wt% B_4C	1900	13.241	76.07	4.4588	1.003
TaC–2 wt% B_4C	2000	13.241	92.3	4.4585	1.001
TaC–2 wt% B_4C	2100	13.241	94.81	4.4584	1.001
TaC–3 wt% B_4C	2100	12.68	97.3	4.4590	1.004

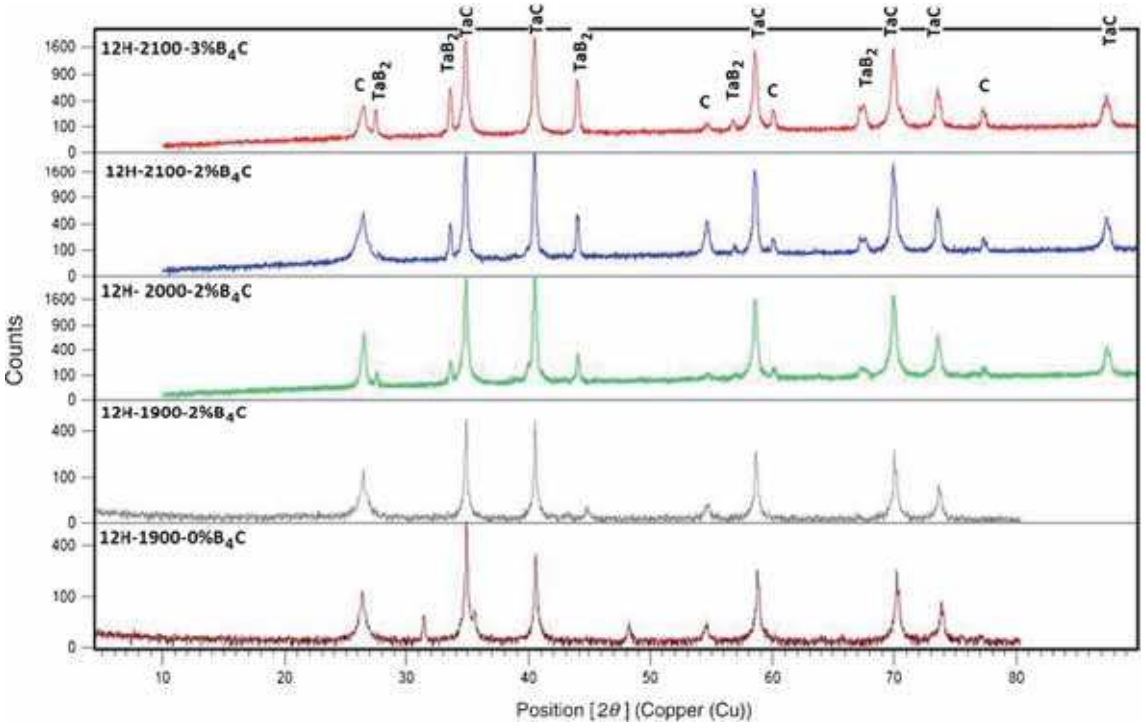

Figure 1. X-ray diffraction patterns of the TaC/TaB_2 composites spark plasma sintered at 1900–2100°C.

Table 3. Mechanical properties of TaC–B_4C composites.

Samples	Sintering temperature (°C)	Vickers' hardness (GPa)	Thickness of the samples (mm)	Flexure strength (MPa)
TaC	1900	14.98	1.2	380
TaC–2 wt% B_4C	1900	15.14	1.1	361
TaC–2 wt% B_4C	2000	15.44	1.0	450
TaC–2 wt% B_4C	2100	16.93	1.2	520
TaC–3 wt% B_4C	2100	16.99	1.4	469

pores were completely closed. Relative density reached 94.8 and 97.3% for 2.0 and 3.0 wt% B_4C, respectively, in 2100°C sintering temperature. B_4C in base materials of these samples formed TaB_2 phase inside TaC grains. Table 2 shows C/Ta ratios for the cubic TaC_y in different materials. The C/Ta values increased with SPS temperature from 1900 to 2000°C. Carbon further dissolving into the TaC_y lattice at higher temperatures was accounted for the C/Ta ratio increase. In addition, elemental impurities such as Ti, Cr, Fe incorporation into TaC_y lattice may also extend the TaC_y lattice, resulting in an over estimation of the C/Ta ratio. However, the largest ratio (C/Ta = 0.9389) calculated for TaC at 1900°C material was still lower than the (C/Ta = 1) predication by reaction (2). This was due to loss of some C by forming CO [8,16]. Samples containing B_4C had C/Ta ratio more than TaC sample. Carbon in B_4C increase C/Ta ratio by dissolving more carbon in TaC lattice. The hexagonal tantalum diboride may also form a substoichiometric TaB_{2-x} instead of stoichiometric TaB_2. In this study, however, the stoichiometry of this hexagonal tantalum diboride phase was not determined due to lack of necessary references [7].

3.2 *Mechanical properties*

The mechanical properties (hardness, flexure strength) of samples are included in table 3. Increase in sintering temperature from 1900 to 2100°C increase hardness of samples. It may be due to increase in density at higher temperature. Increase of B_4C leads to the formation of more TaB_2 phase. Vickers' hardness increased from 14.1 GPa for monolithic TaC to 16.99 GPa for TaC–10 wt% (11 vol%) TaB_2, which was attributed to the higher density achieved for the composite and the higher hardness of the dispersed TaB_2 phase (24.5 GPa) compared with monolithic TaC [8].

The flexure strength of the samples increased with increase in sintering temperature. This factor plays an important role in increasing the density of the samples. The flexure strength of the samples increased with increase in B_4C up to 2.0 wt%,

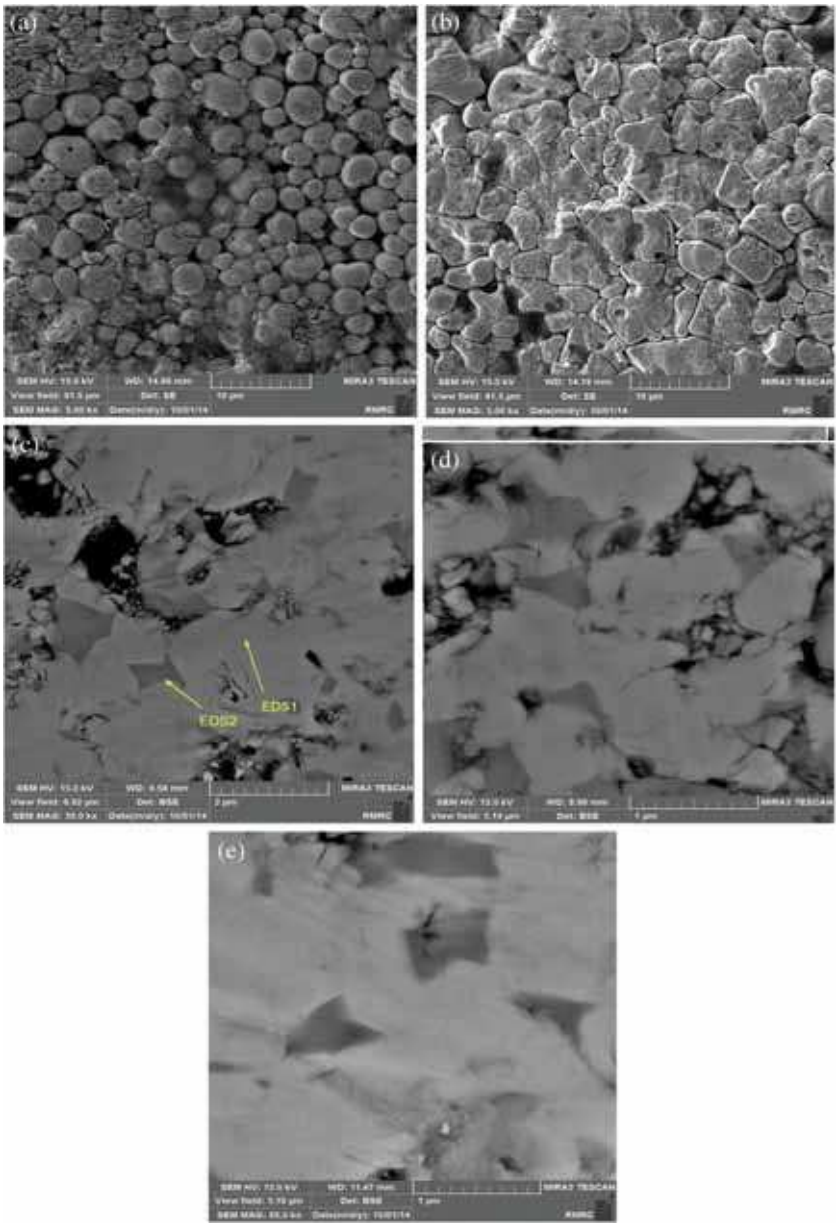

Figure 2. FE-SEM image of sintered samples. (**a**) TaC–0% B_4C, 1900°C; (**b**) TaC–2% B_4C, 1900°C; (**c**) TaC–2% B_4C, 2000°C; (**d**) TaC–2% B_4C, 2100°C and (**e**) TaC–3% B_4C, 2100°C.

but further increases of B_4C reduced the flexural strength composite. Flexure strength of TaB_2 was 600 MPa, with a maximum of 765 MPa and a minimum of 467 MPa. The strength values are comparable to the strength of the monolithic TaC (686 MPa on average). So increase of phase TaB_2 causes reduction in the overall flexure strength of the sample containing 3.0 wt% B_4C.

3.3 *Microstructure development*

FE-SEM analysis of the microstructure of TaC with and without B_4C additions and SPS at various temperatures (figure 2) is included for comparison.

The TaC–TaB_2 composition reached ~76% of the theoretical density after SPS at 1900C or above as shown in table 2. In figure 2c–e, the dark and grey contrasts are attributed to the TaC and the TaB_2 phase, respectively. The bulk densities of TaC–2.0 wt% B_4C sintered by SPS at 1900, 2000 and 2100°C were about 76, 92 and 94%, respectively. The true density was calculated to be 13241 g cm^{-3} using volumetric rule of mixtures and measured composition. For comparison, Zhang *et al* [8] found that the relative densities of the TaC–10 wt% (11 vol%) TaB_2 powder hot pressed at 2100 and 2200°C were 85 and 89% after hot pressing at 2100 and 2200°C, respectively. Enhanced densification of TaC with the TaB_2 addition is likely due to physical pinning

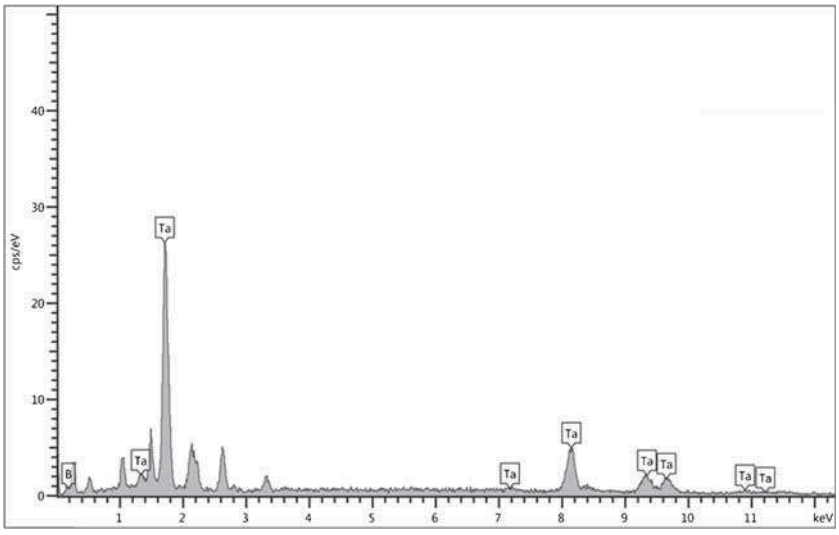

Figure 3. EDS analysis of sample TaC–2% B_4C at 2000°C.

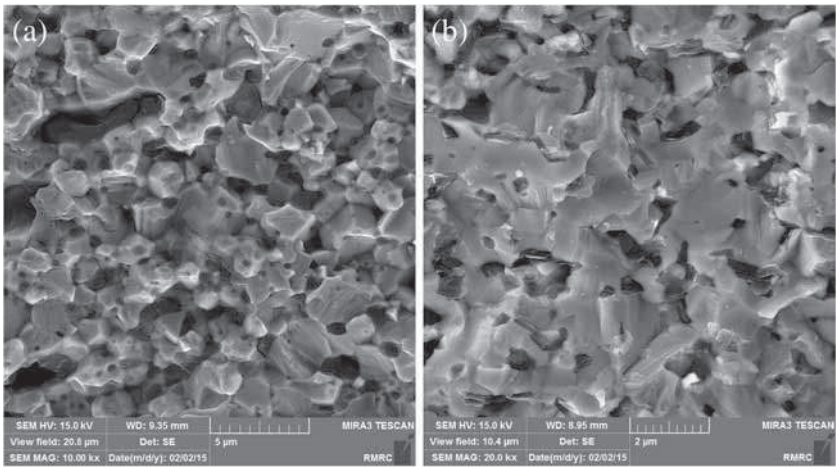

Figure 4. Cross-section of samples (**a**) TaC–0% B_4C at 1900°C and (**b**) TaC–3% B_4C at 2100°C.

of grain growth by the second phase. In addition to grain pinning, the presence of B_2O_3 on the TaB_2 particles' surface may facilitate grain rearrangement due to the formation of a liquid phase, which would enhance densification. A similar grain growth-pinning effect has been observed in the ZrB_2–SiC and HfB_2–SiC systems. In these systems, dispersed SiC particles have been shown to inhibit the grain growth and enhance densification of the matrix phase [8]. With increase in temperature and B_4C up to 3 wt%, the density increased. TaB_2 is also seen in more in TaC phase. The size of the TaC grains could not be determined (in figure 2c–e) because the grain boundaries of TaC could not be distinguished in the polished crosssections. Repeated attempts at thermal etching to reveal the grain boundaries were not successful. Figure 2c–e shows that grain size of newly formed TaB_2 increased by sintering temperature from 400 to 700 nm. EDS analysis of sample TaC–2% B_4C at 2000°C is shown in figure 3.

Cross-section of samples (a) TaC–0%B_4C at 1900°C and (b) TaC–3% B_4C at 2100°C is shown in figure 4. The size of the TaC grains in sample TaC–0% B_4C at 1900°C is 2–3 micron and size of the TaC grains in sample TaC–3% B_4C at 2100°C is 300 to 500 nm.

4. Conclusion

TaC–B_4C powder was sintered by spark plasma sintering at temperatures ranging from 1900 to 2100°C, achieving a relative density of 66.0% at 1900°C and a 30 MPa applied pressure without the use of sintering additives. B_4C additive was subsequently used to react with TaC powder. The onset temperature for densification of TaC was lowered through the use of B_4C additive. TaC with 2.0 wt% B_4C additions could be sintered to 94.8% density at 2100°C with minimal grain growth and mostly intergranular porosity. Increase in B_4C up to 3.0 wt% increases the relative

densification up to 97.3% and the hardness of samples to 16.99 GPa. Flexure strength of the sample containing 2.0 wt% B_4C increased up to 520 MPa and in future increasing B_4C up to 3.0 wt%, flexure strength of the sample reduced because flexure strength of TaB_2 balk is lower than TaC.

Acknowledgements

We are indebted to material department in Malek-e-Ashtar University of Technology, which supplied the raw materials for the development of this research and to building and construction department of Standard Research Institute for its equipment support.

References

[1] Liu L, Yea F, Hea X and Zhoua Y 2011 *Mater. Chem. Phys.* **126** 459

[2] Mehdikhani B and Bakhshi S R 2014 *J. Optoelectronic Adv. Mater.* **16** 1311

[3] Wuchina E, Opila E, Opeka M, Fahrenholtz W and Talmy I 2007 *Electrochemical Society Interface* **16** 30

[4] Johnson M, Gasch M and Lawson J W 2008 *Am. Inst. Aeronautics Astronautics*

[5] Justin J F and Jankowiak A 2011 *Onera J. Aerospace Lab* **3** 1–11

[6] Samonov G V and Petrikina R Y 1970 *Phys. Sinter.* **2** 1

[7] Zhang X, Hilmas G E and Fahrenholtz W G 2008 *J. Am. Ceram. Soc.* **91** 4129

[8] Zhang X, Hilmas G E and Fahrenholtz W G 2007 *J. Am. Ceram. Soc.* **90** 393

[9] Liu J X, Kan Y M and Zhang G J 2010 *J. Am. Ceram. Soc.* **93** 370

[10] Kim B, Woo K, Doh J, Yoon J and Shon I 2009 *Ceram. Int.* **35** 3395

[11] Shen Z, Johnsson M, Zhao Z and Nygren M 2002 *J. Am. Ceram. Soc.* **85** 1921

[12] Sommer M, Schubert W D, Zobetz E and Warbichler P 2002 *Int. J. Refract. Metal Hard Mater.* **20** 41

[13] Khaleghi E, Lin Y S, Meyers M A and Olevsky E A 2010 *Scripta Materialia* **63** 577

[14] Silvestroni L, Bellosi A, Melandri C, Sciti D, Liu J and Zhang G 2011 *J. Eur. Ceram. Soc.* **31** 619

[15] Mehdikhani B and Borhani G H 2014 *J. Optoelectronic Adv. Mater.* **16** 524

[16] Talmy I G, Zaykoski J A and Opeka M M 2010 *Eur. Ceram. Soc.* **30** 2253